

## EARTHQUAKE-RESISTANT DESIGN OF SALMAN FARSI ARCH-GRAVITY DAM

Dr. M. Wieland and Dr. S. Malla

Electrowatt Engineering Services Ltd., Zurich, Switzerland

Dr. V. Lotfi and G. Khoshrang

Mahab Ghodss Consulting Engineers, Tehran, Iran

### ABSTRACT

The design aspects of the 125 m high Salman Farsi (Ghir) arch-gravity dam in Iran, which is governed by earthquake loads, are discussed. The dam is located in the seismically very active foothills of the Zagros Mountains. The methodology used for seismic shape optimization is explained which includes the arrangement of the crest spillway and selection of the overall stiffness of the dam. The dam on massless foundation is analysed for the operating basis earthquake, taking into account compressibility of the reservoir and energy absorption at the reservoir bottom. Floor response spectra are given for the central crest spillway, where the maximum spectral accelerations for 5% damping reach values of up to 6 g compared to that of the ground motion of 0.7 g.

### 1. INTRODUCTION

For the earthquake-resistant design of concrete dams, the stress criteria for the operating basis earthquake (OBE) have to be satisfied primarily. For the seismic safety check, where concrete cracking is accepted as long as this does not lead to uncontrolled release of water from the reservoir, the maximum credible earthquake (MCE) is relevant. Well-designed arch and arch-gravity dams can usually withstand the MCE if they can resist the OBE without structural cracks and if the foundation rock does not fail prematurely. This is true even for dams in zones of very high seismicity such as Iran. Therefore, attention has mainly to be paid to the OBE in the design process (Lotfi et al., 1995). Safety evaluations of existing arch dams have been reported by Lotfi et al. (1992), Razavi et al. (1992), Wieland and Lotfi (1993) and Wieland (1994), where the dynamic stability under the MCE has been checked using rigid body models of detached cantilever blocks for ground accelerations of up to 0.5 g. A dynamic stability analysis of the Sefid Rud buttress dam has also been reported by Ahmadi and Khoshrang (1992) to assess the sliding and overturning safety of the top portion of cracked buttresses (Fig. 1) following the June 21, 1990 Manjil earthquake in the northwest of Iran (magnitude: 7.5). To improve the seismic stability of detached blocks, post-tensioning cables have been provided. In two other arch dam projects reported by Tardieu et al. (1992), a so-called aseismic belt has been provided near the dam crest in order to improve the dynamic stability of the upper portion of the dam which undergoes the highest earthquake stresses. The aseismic belt is made of ductile steel bars.

Seismic strengthening is also known from the Hsinfengkiang buttress dam in China and the Koyna gravity dam in India. In these well-known cases of reservoir-induced seismicity, concrete was added to change the dynamic properties of the damaged dam as well as to reduce the seismic stresses.

Little is reported in the literature about the earthquake-resistant design of concrete dams. Usually a design is made based on the local site conditions and the way the water load is transferred to the foundation rock. Once an appropriate dam layout and shape have been selected, it is checked if the earthquake stresses are also within the allowable limits. The design of the dam, however, is usually not altered because of the vibratory effect of the earthquake ground shaking. The situation looks different if an active fault passes through the foundation of a dam. Two cases are known (Hatton et al., 1987 and Gilg et al., 1987) where fault movements had to be accommodated by concrete dams.

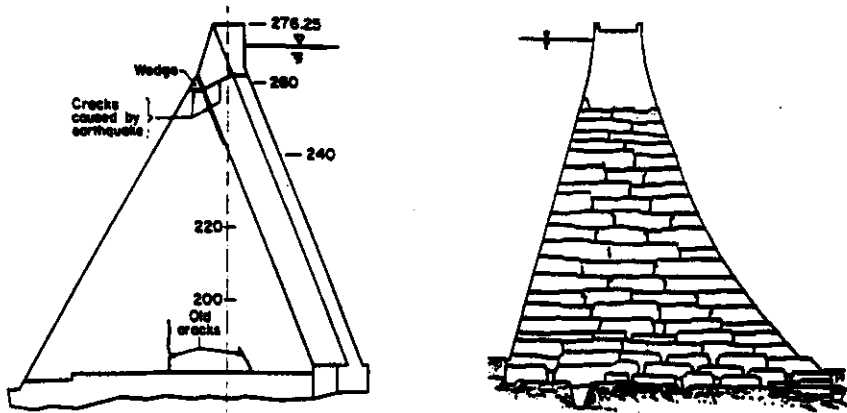


Fig. 1 Main cracks caused by 1990 Manjil earthquake in buttress no. 15 of Sefid Rud buttress dam (Iran) and sketch of interlocking blocks of Lower Crystal Springs gravity dam (USA)

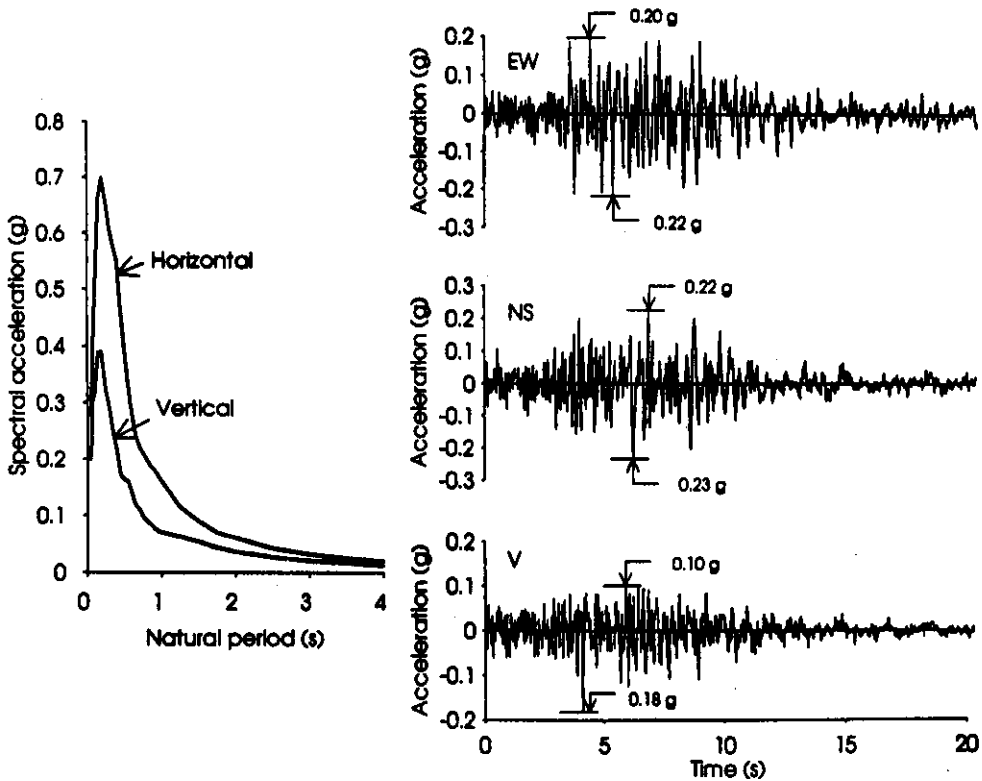


Fig. 2 Design response spectra for 5% damping of operating basis earthquake and spectrum-compatible accelerograms for the three components of ground motion (accelerograms recorded at Griffith Park Station, San Fernando earthquake 1971, were modified)

The question remains: which dam type is most suited to resist strong earthquakes and what is its shape? As mentioned earlier there are factors other than the local conditions which govern the earthquake safety of a concrete dam. The guiding principles which apply almost universally are:

- symmetry and simplicity;
- uniform distribution of stiffness and mass;
- uniform strength;
- not too elongated in plan (to minimize the effect of non-uniform ground motion);
- no stress concentrations;
- ductility and damping; and
- high stiffness in crest region.

Among these principles, the last two need further explanation. What is the ductility of an unreinforced concrete arch dam? The ductility of the dam is its post-cracking behaviour and covers the range between the full development of cracks and the limits of dynamic stability of detached concrete blocks. Therefore, to achieve ductility, brittle shear failure mechanisms have to be avoided in the dam-foundation contact zone. As a matter of fact, cracks in a dam may not be detrimental to the earthquake safety of a dam. The 57 m high Lower Crystal Springs gravity dam, whose crest is slightly curved in plan and which is located very close to the San Andreas fault, survived the powerful 1906 San Francisco earthquake with no damage. The dam shown in Fig. 1 is made of a large number of interlocking concrete blocks. The friction in the joints and the block interlock prevented joint movements. A similar mechanism is expected for the detached cantilevers of an arch or arch-gravity dam.

The other point is the high stiffness in the crest region of an arch dam which is necessary to reduce the deflections and accelerations in that zone and to increase the frequencies of the lowest modes of vibrations. It is well known from shell theory that a strong shell can be achieved when the applied loads are carried by membrane forces and not in bending. Large bending stresses and corresponding deflections occur along the free boundary of a shell, i.e. along the crest in an arch dam. The stiffening of the crest is, therefore, the most efficient means in changing the dynamic properties of a dam. Accordingly, the location of a large crest spillway will also affect the fundamental mode shapes considerably.

The other principles will be discussed in the subsequent part.

## 2. DESIGN EARTHQUAKE MOTION

The peak values of the horizontal and vertical components of the ground acceleration of the OBE have been estimated as 0.26 g and 0.17 g respectively. The average return period of the OBE is about 145 years. The smooth design response spectra, determined based on a comprehensive seismic hazard study, are shown in Fig. 2 together with the spectrum-compatible acceleration time histories for the three components of the ground motion at the site. As a basis for these accelerograms, the accelerograms recorded at the Griffith Park Station during the 1971 San Fernando earthquake were used. In an iterative procedure, the acceleration amplitudes were modified so that acceptable agreement could be reached between the modified Griffith Park Station spectra and the given target spectra for 5% damping.

## 3. STRUCTURAL MODELLING

The three-dimensional finite element model of the dam-reservoir-foundation system shown in Fig. 3 has been used for all dynamic analyses. The main assumptions are as follows:

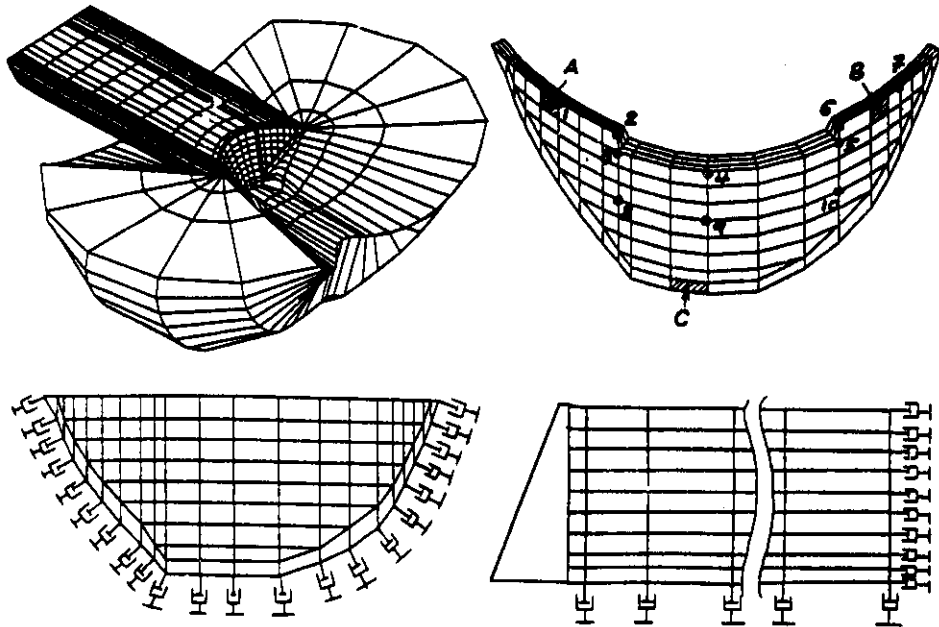


Fig. 3 Three-dimensional finite element model of dam-reservoir-foundation system of Salman Parsi arch-gravity dam, reservoir model with energy-absorbing dampers, and location of nodal points and elements where the dynamic responses are given in Tables 1 and 2

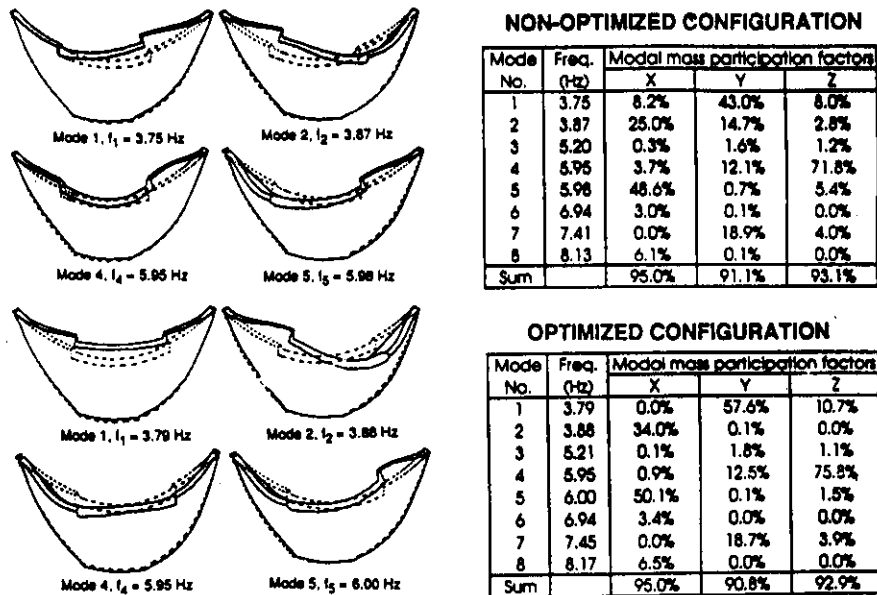


Fig. 4 Eigenfrequencies, modal mass participation factors and mode shapes of non-optimized and optimized dam configurations (effect of location of crest spillway on dynamic characteristics of dam); X-, Y- and Z-directions are respectively across-stream, along-stream and vertical directions

- massless foundation (inertial effects in the foundation and dam-foundation interaction effects are neglected);
  - uniform ground motion with two horizontal and one vertical components acting simultaneously;
  - linear-elastic behaviour of mass concrete, rock and the compressible water in the reservoir; and
  - small strains and displacements.
- Energy radiation at the far end of the infinite prismatic reservoir and energy absorption at the reservoir bottom are accounted for by viscous dampers according to Lysmer and Kuhlemeyer (1969).

#### 4. DYNAMIC MATERIAL PROPERTIES

For the dynamic analyses, the moduli of elasticity of mass concrete and rock were taken as 30 GPa and 14.4 GPa respectively. Structural damping was modelled by Rayleigh damping with a damping ratio of 6% at the frequencies of 4 Hz and 10 Hz, i.e. the first two modes of the system with full reservoir with eigenfrequencies of 3.0 Hz and 3.2 Hz have damping ratios of about 7% and the other modes with frequencies in the range of 4 Hz to 10 Hz have damping ratios between 5% and 6%. The relatively high damping ratios of about 7% for the first two modes are acceptable in view of the energy radiation from the massive arch-gravity dam into the foundation rock.

The impedances of the viscous dampers per unit area, i.e. the product of P-wave propagation speed and mass density, at the far end of the reservoir and over the reservoir bottom are taken as  $1.43 \times 10^6$  kg/m<sup>2</sup>s and  $4.29 \times 10^6$  kg/m<sup>2</sup>s respectively. The mass densities of water and rock of the reservoir bottom are 1000 kg/m<sup>3</sup> and 2400 kg/m<sup>3</sup> respectively, and the corresponding P-wave propagation velocities are taken as 1430 m/s and 1790 m/s respectively. The latter value also takes into account the energy absorption at the reservoir bottom by sediments.

#### 5. EARTHQUAKE-RESISTANT DESIGN

As pointed out earlier, earthquake-resistant design calls for dynamic optimization of the dam which is quite different from static optimization. The objective function for dynamic optimization can be expressed in terms of uniform distribution of earthquake stresses (no stress concentrations), simplicity, i.e. easy and clear understanding of the dynamic behaviour of the dam (this is only possible when the dominant mode shapes are either symmetrical or antisymmetrical), and high stiffness of the crest region. A quantification of these rather fuzzy objectives is difficult. The best approach consists of a trial and error procedure based on engineering judgement during which the overall dam volume, which has been determined based on static loads, remains unchanged.

In the case of the Salman Farsi dam, the crest region was stiffened. The location of the spillway, which was initially determined based on hydraulic considerations only, was shifted. Filets were provided along the abutments to reduce the stress concentrations along the dam-foundation contact, and the thickness profile of the cantilevers was changed. The result of this optimization was satisfactory as shown in Fig. 4, where a comparison is made between the dynamic properties with the first proposed location and the final dynamically optimum location of the spillway. The other factors mentioned above were kept the same in this comparison. We can notice from the modal mass participation factors that a relatively small shift of the spillway from the optimum position leads to complicated coupled vibrations which can be excited by any component of the ground motion. In that case, the behaviour of the dam can only be understood by computer simulation, whereas in the optimum case, an engineer is able to readily understand the behaviour of the dam during an earthquake. A comparison of the original (non-optimized) dam with the optimized one has shown that the maximum dynamic tensile stresses are roughly 50% smaller in the optimized dam.

## 6. EARTHQUAKE ANALYSIS

The Salman Farsi dam has been analyzed for the cases with an empty reservoir and with a full infinite compressible reservoir with and without energy absorption along the reservoir bottom. The calculations were carried out with the computer program ADINA using direct time integration with a time step of 0.02 s. In the dynamic analysis with the OBE, emphasis was put on the maximum displacement and acceleration responses along the dam crest. The results for the three cases are compared in Tables 1 and 2. Some earthquake responses with the full reservoir using models with and without energy absorption at the reservoir bottom are compared in Figs. 5 to 8. The maximum relative displacement and relative acceleration at the crest are 25 mm and 1.8 g respectively for the empty reservoir case; for the full reservoir condition, the maximum values are 36 mm and 1.4 g respectively when the bottom energy absorption is ignored, and 27 mm and 1.1 g respectively when it is considered. From Tables 1 and 2, it is clear that the consideration of energy absorption at the reservoir bottom leads to a reduction of up to 30% in the dynamic response.

To understand better the inertial forces acting in the spillway region, the floor response spectra at three critical points on the crest have been calculated for a damping ratio of 5% (Fig. 7). The spectra have been calculated from the time histories of absolute accelerations. Figure 6 shows that amplification factors of up to 5 (full reservoir) are possible in the absolute acceleration response at the dam crest with respect to the peak ground acceleration of 0.26 g. We can notice in Fig. 7 that the maximum spectral acceleration is about 6 g for the OBE. Therefore, if a component on the crest or a part of the crest spillway has an eigenfrequency close to the first or second eigenfrequency of the dam, very large earthquake forces will occur even under the effect of the OBE which may damage this component. The only way to cope with these forces is by means of detuning the critical components. That can be achieved by seismic isolators (elastomeric bearings), stiffening of the component or by special damping elements. In most dams, the designers of the electromechanical equipment have used the acceleration spectra on ground, rather than the floor response spectra. Such an approach will lead to a dangerous overestimate of the earthquake safety of any central crest spillway and any components located on or near the dam crest. Therefore, for the seismic design of the electromechanical equipment, a method must be applied which is compatible with the dynamic behaviour of the dam. This has been the normal practice in the design of nuclear plant facilities.

## 7. SENSITIVITY OF RESULTS OF DYNAMIC ANALYSIS

Every strong earthquake is different from all others. Therefore, to rely completely on a given design response spectrum or a set of recorded accelerograms is dangerous if the design is only oriented towards fulfilment of the allowable stress criterion. We have to bear in mind that the accuracy of the results of a dynamic analysis depends on a number of factors such as:

- Deviation of acceleration response spectra of spectrum-compatible accelerograms from the target spectra: The maximum deviation is estimated at about 30%.
- Accuracy of finite element mesh and type of finite elements: Considerable errors have to be expected at locations of stress concentration, i.e. at corners of crest spillway and along the dam-foundation contact.
- Accuracy of numerical integration method: A reduction of the time step from 0.02 s to 0.01 s can affect the peak values of the dynamic response by up to 10%.
- Modelling of the reservoir: There is still a considerable difference between the results obtained from analyses with compressible and incompressible reservoirs, and reservoirs with and without energy absorption at the bottom, resulting in deviations of up to 40%.

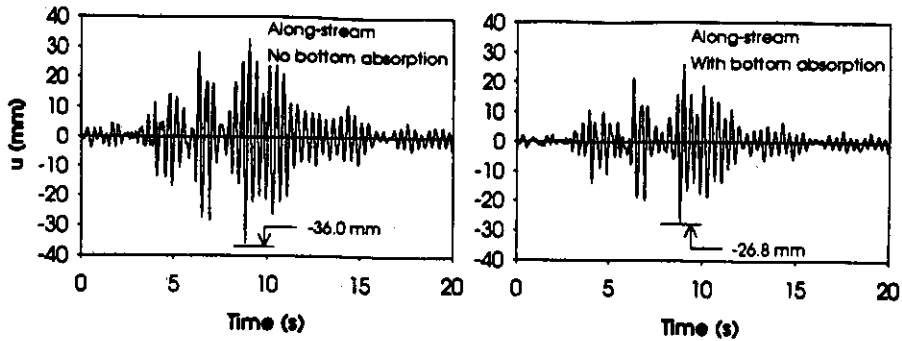


Fig. 5 Time histories of relative displacement in up-/downstream direction at crest of crown cantilever of dam with full reservoir for models with and without energy absorption at reservoir bottom

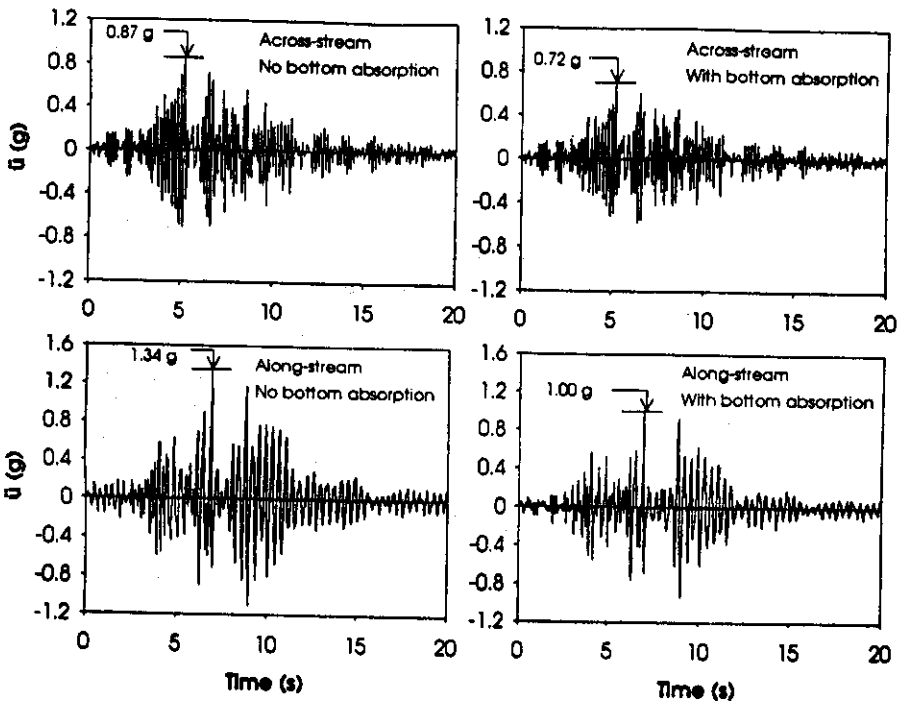


Fig. 6 Time histories of across- and along-stream components of absolute acceleration at crest of crown cantilever of dam with full reservoir for models with and without energy absorption at reservoir bottom

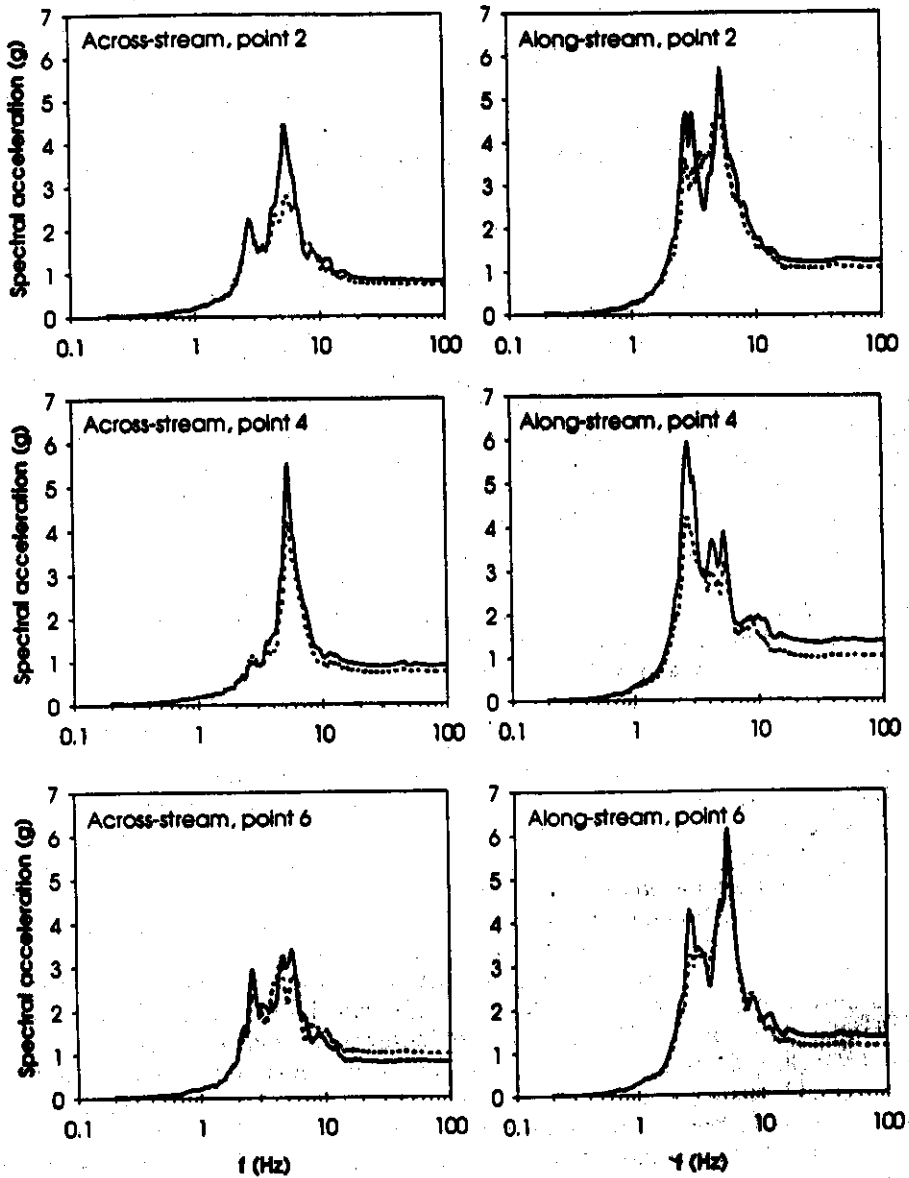


Fig. 7 Floor response spectra for 5% damping at selected points shown in Fig. 3 along crest spillway of dam with full reservoir for models with (dashed line) and without (full line) energy absorption at reservoir bottom



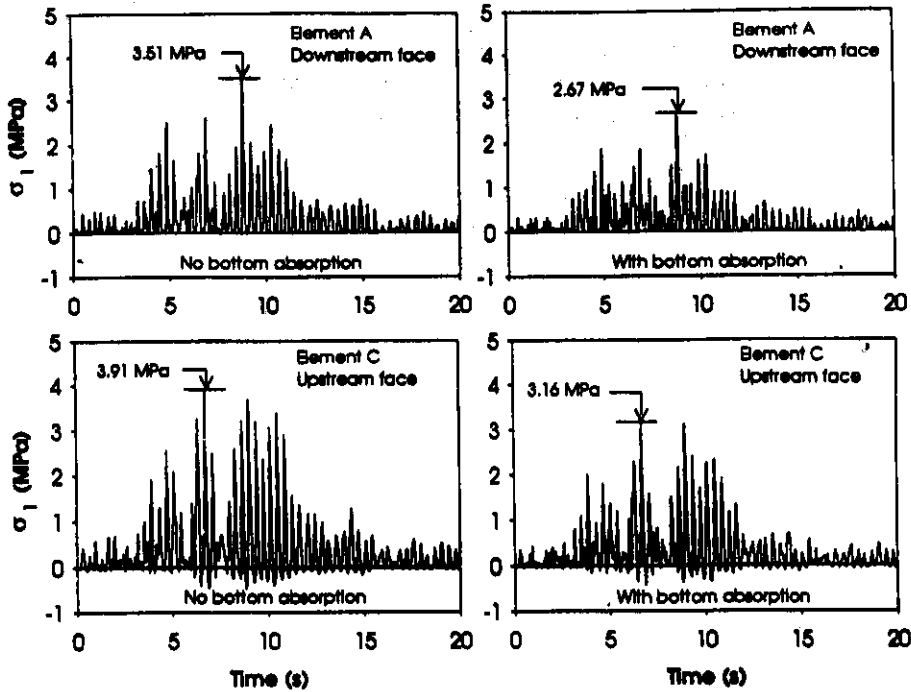


Fig. 8 Time histories of principal dynamic tensile stresses at crest quarter point on downstream face and at base of upstream face of dam with full reservoir for models with and without energy absorption at reservoir bottom

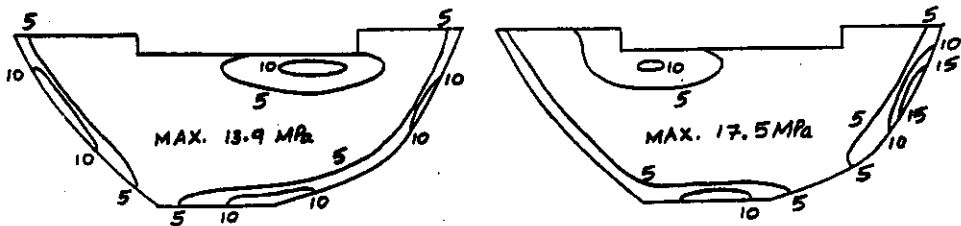


Fig. 9 Plots of required strength of mass concrete at upstream face of dam for a load combination comprising dead load, water load and OBE showing effect of choice of cross-canyon earthquake component; results in right figure were obtained by reversing the sign (multiplying by -1.0) of the input accelerogram of cross-canyon component used in left figure

- Accuracy of material properties: The greatest uncertainties are with respect to the damping properties of the dam and the foundation. Actual measurements indicate damping ratios ( $\xi$ ) in the range of 2% to 3%, while in dynamic analyses values between 5% to 10% are used. The effect of variation in the damping ratio can be estimated as follows (Newmark and Hall, 1978):

$$c(\xi) = 0.0394 - 0.3414 \ln \xi \quad (\text{acceleration, stress})$$

$$c(\xi) = 0.4315 - 0.2021 \ln \xi \quad (\text{displacement})$$

where  $c(\xi)$  is a damping-dependent correction factor which has a value of 1.0 for a damping ratio of 0.06. For  $\xi = 0.03$ , the stresses are about 20% to 25% larger than for  $\xi = 0.06$ .

To cope with these errors, it is necessary that the dam has extra strength and stability. Fortunately, there exists a wide margin between the accelerations causing initial cracking in a dam and those leading to failure of detached concrete blocks. In view of the above uncertainties, it is too costly and not practical to design a dam elastically as long as it can be guaranteed that the dam can withstand the MCE. Friction in contraction joints and cracks, and block interlock ensure that well-built dams can resist the effects of strong earthquake ground shaking.

## 8. SELECTION OF CONCRETE STRENGTH

The last step in the earthquake-resistant design of a dam is the selection of the concrete strength based on the results of the static and dynamic analyses. For all relevant load combinations, the concrete strength is computed based on the conventional biaxial strength curve of mass concrete. In general, the concrete strength is determined by either the biaxial tension or the combined tension-compression stress state. For the usual static loads, a safety factor of 2 is required for biaxial tensile stresses and a factor of 3 for biaxial compressive stresses. Under earthquake loads (OBE), following the previous discussion on the accuracy of the results of a dynamic analysis, a safety factor of 1.5 is required for the tensile stresses. The dynamic compressive stresses are not a problem for arch-gravity dams. To compute the concrete strength, the following relation between the static tensile ( $f_t$ ) and compressive strength ( $f_c'$ ) is used:

$$f_t = 0.29 |f_c'|^{2/3} \quad (f_t \text{ and } f_c' \text{ in MPa}) \quad (1)$$

For the earthquake load case, it is assumed that the OBE occurs when the mass concrete is at least 5 years old. This means that an increase in the 28-day concrete strength of approximately 40% can be assumed due to the age effect. Moreover, the tensile strength is assumed to be 30% larger under earthquake loads than under static loads. For example, using the above factors, an earthquake stress of 4 MPa (biaxial tension) would require a 28-day uniaxial compressive strength of 45.5 MPa, taking into account a tensile stress safety factor of 1.5.

Typical strength contour plots following this procedure are shown in Fig. 9 for the OBE load combination, using, however, a tensile stress safety factor of 1.0. We can notice that the required strength plots for the OBE are highly asymmetric. This is due to the large influence of the cross-canyon component of the ground motion and the fact that the maximum stress response is due to a single stress pulse. Reversal of the sign of the cross-canyon accelerogram, i.e. multiplying all values by -1.0, results in a significant change in the required strength plots as shown in Fig. 9. This result indicates that the selection of the concrete strength very much depends on the nature of the selected ground motion. Therefore, the engineer must be careful in selecting the concrete strength based on the dynamic stress response of the dam. In the examples shown in Fig. 9, the maximum required 28-day concrete strength is 17.5 MPa.

We would also like to point out that the dynamic tensile strength of mass concrete in a large dam cannot be much higher than about 4 MPa, due to the size effect. In the grouted contraction joints, these values are considerably smaller.

## 9. DYNAMIC STABILITY

The dynamic stability of the dam must be checked for the MCE. In the selection of the MCE, even higher uncertainties are involved compared to the case of the OBE. Therefore, an earthquake-proof dam must be able to withstand ground motions with intensities which greatly exceed those of the OBE. Once the OBE is exceeded, cracks will develop in the dam. In that case, the dam is held together effectively by joint friction, block interlock and the arch stresses due to the water load and the contraction joint grouting. As shown by Malla and Wieland (1995), joint movements to be expected during a strong earthquake will be very small, i.e. detached cantilever blocks are unlikely to fall down.

The main question for a dam engineer with regard to earthquakes is: what type of concrete dam is most suitable to resist strong ground shaking? From the point of view of dynamic stability, it is either a gravity dam which is slightly curved in plan or an arch-gravity dam. In both cases, the integrity of detached blocks is improved by arch stresses due to the water load. Thin arch dams in wide valleys are less suitable because of possible brittle shear failure at the dam-foundation contact zone and because of the larger accelerations in the central upper portion of the dam. Moreover, once the arch stresses have been relieved, there is little resistance due to load redistribution (load bearing by cantilevers). However, gravity or arch-gravity dams could carry the water load by cantilever action.

## 10. CONCLUSIONS

Based on the results of the extensive dynamic analyses carried out for the Salman Farsi arch-gravity dam, the following conclusions can be drawn:

1. For the earthquake-resistant design, the stresses during the OBE must be within acceptable limits; in that case, the dynamic stability of a well-designed arch dam under the MCE is usually also satisfied.
2. The main criteria for dynamic dam shape optimization are: large stiffness of dam crest and symmetry of the lowest modes of vibration.
3. Any earthquake analysis includes considerable uncertainties; therefore, a conservative approach has to be adopted in the aseismic design.
4. The maximum dynamic tensile stress in the dam under the OBE is 4.0 MPa, the maximum up-/downstream deflection is 36 mm, and the maximum relative crest acceleration is 1.4 g with a full reservoir without bottom absorption; with an empty reservoir, the maximum relative crest displacement and acceleration are 25 mm and 1.8 g respectively.
5. The maximum spectral acceleration at the crest is about 6 g (5% damping).
6. The inclusion of the energy absorption at the reservoir bottom in the finite element model reduces the maximum dynamic response by up to 30%.

## REFERENCES

- Ahmadi, M.T. and Khoshrang, G. (1992). Sefid Rud Dam's Dynamic Response to the Large Near-field Earthquake of June 1990. *Dam Engineering*, Vol. III, Issue 2, May 1992.
- Gilg, B. et al. (1987). Special Design of Steno Arch Dam in Greece in Relation with Possible Fault Movements. Proc. ICOLD Symp., Beijing, 1987.
- Hatton, J.W., Black, J.C. and Foster, P.F. (1987). New Zealand's Clyde Power Station. *Water Power & Dam Construction*, Dec. 1987.

- Lotfi, V., Mokhtar-Zadeh, A., Sadeghifard, H., Arasteh, T. and Wieland, M. (1992). Behaviour of Karun I Arch Dam in Iran under the Maximum Credible Earthquake. Proc. Int. Symp. on Arch Dams, Nanjing, China.
- Lotfi, V., Khoshrang, G., Malla, S. and Wieland, M. (1995). Seismic Analysis and Earthquake-Resistant Design of Arch-Gravity Dam. Proc. 2nd Int. Conf. on Seismology and Earthq. Engng. (SEE-2), Tehran, Iran, May 15-17, 1995.
- Lysmer, J. and Kuhlemeyer, R.L. (1969). Finite Dynamic Model for Infinite Media. J. Eng. Mech. Div., ASCE, EM4.
- Malla, S. and Wieland, M. (1995). Effect of Friction in Vertical Contraction Joints of Arch Dam. Proc. Symp. on Research and Development in the Field of Dams, Crans-Montana, Switzerland, Sept. 7-9, 1995.
- Newmark, N.M. and Hall, W.J. (1978). Earthquake-resistant Design of Nuclear Power Plants. The Assessment and Mitigation of Earthquake Risk, UNESCO, 1978.
- Razavi, S., Lotfi, V., Arasteh, T., Wieland, M. and Guimond, R. (1992). A Re-Analysis of Dez Arch Dam in Iran. Proc. Int. Symp. on Arch Dams, Nanjing, China.
- Tardieu, B. et al. (1992). New Developments in the Seismic Analysis of Dams. Civil Engineering Structures and Industrial Facilities, pp. 547-585.
- Wieland, M. and Lotfi, V. (1993). Seismic Safety Evaluation of a 200 m High Arch Dam under Maximum Credible Earthquake. Proc. Int. Workshop on Dam Safety Evaluation, Grindelwald, Switzerland.
- Wieland, M. (1994). Earthquake Safety of Concrete Dams. State-of-the-Art Paper, Proc. 10th European Conference on Earthquake Engineering, Vienna, Austria.

Table 1 Absolute maximum relative displacements and relative accelerations in up-/downstream direction for empty and full reservoir conditions with and without energy absorption at reservoir bottom (locations of reference points are shown in Fig. 3)

Point	Empty reservoir		Full reservoir			
			No bottom absorption		With bottom absorption	
	Displ. (mm)	Accel. (g)	Displ. (mm)	Accel. (g)	Displ. (mm)	Accel. (g)
1	11.5	0.92	14.5	0.66	10.9	0.67
2	19.0	1.66	28.4	1.22	19.7	1.08
3	14.1	1.21	22.9	0.88	16.2	0.74
4	19.5	1.43	36.0	1.38	26.8	1.03
5	19.5	1.38	21.9	0.95	17.6	0.85
6	24.6	1.77	26.8	1.28	22.4	1.12
7	9.6	0.76	10.3	0.53	8.4	0.43
8	5.7	0.49	9.7	0.43	7.1	0.38
9	10.3	0.75	15.0	0.65	11.2	0.53
10	7.9	0.60	9.1	0.39	7.1	0.37

Table 2 Absolute maximum principal dynamic stresses in MPa at up- and downstream faces of selected elements shown in Fig. 3 for empty and full reservoir conditions with and without energy absorption at reservoir bottom.

Case	Upstream face			Downstream face		
	A	B	C	A	B	C
Empty reservoir	1.34	1.85	2.96	1.85	1.99	1.59
Full reservoir: no bottom absorption	2.08	2.08	4.01	3.51	3.13	2.07
Full reservoir: with bottom absorption	1.51	1.65	3.16	2.67	2.67	1.73